Single molecules detect ultra-slow oscillators in a molecular crystal excited by ac-voltages

Kolchenko, M.A.; Nicolet, A.A.L.; Galouzis, M.D.; Hofmann, C.; Kozankiewicz, B.; Orrit, M.A.G.J.

Single molecules detect ultra-slow oscillators in a molecular crystal excited by ac voltages

2009 New J. Phys. 11 023037

(http://iopscience.iop.org/1367-2630/11/2/023037)

New Journal of Physics
The open-access journal for physics

Single molecules detect ultra-slow oscillators in a molecular crystal excited by ac voltages

M A Kol'chenko[1,2], A A L Nicolet[1], M D Galouzis[1], C Hofmann[1], B Kozankiewicz[3] and M Orrit[1,4]

[1] MoNOS, Huygens Laboratory, Leiden University, 2300RA Leiden, The Netherlands
[2] Institute for Spectroscopy, Russian Academy of Sciences, 142190 Troitsk, Moscow Region, Russian Federation
[3] Institute of Physics, Polish Academy of Sciences, 02–668 Warsaw, Poland
E-mail: orrit@molphys.leidenuniv.nl

New Journal of Physics **11** (2009) 023037 (22pp)
Received 29 September 2008
Published 20 February 2009
Online at http://www.njp.org/
doi:10.1088/1367-2630/11/2/023037

Abstract. We monitored the spectral shifts of single molecule lines under an applied ac voltage in a molecular crystal at a low temperature. When varying the voltage modulation frequency, we found pronounced resonances in the oscillating shift of the optical lines. The resonance frequencies are surprisingly low and are found anywhere in the explored region, from some tens of kHz to a few MHz. Their width and amplitude depend very steeply on temperature, with quality factors as high as a few hundred at 1.4 K. Probing the resonant modes with single molecules at different locations, we find a clear spatial correlation of the modes within microcrystalline domains, extending over 10–100 μm. For large amplitudes, the oscillations become anharmonic and display a range of nonlinear effects: decrease of the frequency with amplitude, hysteretic behavior depending on the scan direction and shift of the frequency when an external strain is applied to the sample. Put together, our observations point to low-frequency acoustic modes localized at or around crystal defects. This work is closely related to earlier observations of similar resonances in Shpol'skii matrices deposited on a semiconductor. We speculate on the relation of these acoustic modes to the low-energy modes (quasi-localized modes and Boson-peak excitations) already known in disordered solids.

[4] Author to whom any correspondence should be addressed.

Contents

1. Introduction

Single-molecule (SM) optical signals are attractive probes of the local conditions around each molecule [1]. The present work was initiated as a search for local electric fields and charge distributions in a molecular crystal where fluorescent impurity molecules (nanoprobes) are dispersed at a low concentration [3]–[5]. Electric fields are applied to the sample by means of metallic electrodes, and may affect SM lines either directly through the well-known Stark effect [6] or by charge injection at electrode–crystal contacts. The resulting time-dependent charge distribution creates additional fields, which in turn can affect SM lines. At low temperature, the first mechanism (hereafter called the Stark effect) is assumed to arise mostly from the electronic polarizability, and is therefore expected to be comparatively weak but very fast. Its response time should lie in the optical frequency region [6], practically instantaneous on the time scale of electronic detection events. The Stark effect has been used in the past to modulate SM lines at frequencies as high as several hundreds of MHz [6]–[9]. The second effect, which results from charge injection, can be very strong and very slow. It is much more complex, as it depends on the full geometry (because of the long range of Coulomb forces), defect distribution and history of the sample. Slow relaxation of optical lines has been observed by Bauer and Kador [10, 11] and, more recently, by us in field-effect transistor (FET) structures similar to those used hereafter, where charge injection took place [12, 13].

Charge injection depends in a critical way on electrical contact and varies considerably from sample to sample. In the present paper, we consider only samples in which charge injection remained limited, at least in the region where the SMs are located. Therefore, the weak and fast Stark effect was assumed to dominate SM optical shifts. Surprisingly, on applying ac voltages of a few volts to our structures, we observed resonant responses at frequencies as low as some tens of kilohertz. Those ultra-slow resonances are reminiscent of earlier observations done with SMs in an n-alkane matrix covering a semiconductor substrate, in which an oscillating current was circulated [14, 15]. Although these phenomena had been tentatively attributed to one of several possible electrical effects [14, 15], the new experiments reported here suggest that this interpretation was incorrect, and that the origin of these oscillations is in fact acoustical or mechanical.

Localized acoustic oscillations in solids are often quickly damped by coupling to delocalized acoustic phonons in substrates or supporting structures. Well-known exceptions are

surface acoustic waves in periodic structures, tuning forks, resonators and cantilevers often designed, optimized and constructed for use as frequency standards or as probes in atomic force microscopy. To our knowledge, the accidental appearance of ultra-slow localized acoustic modes with high-quality factors in a molecular crystal is reported here for the first time. Our observations suggest that these oscillators may be more common than was realized up to now, and may play an important part in the thermal and dissipative properties of disordered solids at low temperature. These modes may be considered as belonging to the extreme low-frequency tail of the distribution of soft vibration modes currently observed with other techniques in glasses, imperfect crystals and other disordered systems, and known as quasi-local modes or Boson peak excitations. Although these oscillators are still impossible to design and construct in a controlled way, they may constitute interesting models for a variety of nanomechanical and electromechanical devices.

The outline of this paper is as follows: section 2 describes the sample preparation and the experimental procedures we employed. The results of a variety of experiments done on these oscillators are discussed in section 3. Section 4 is devoted to a discussion of possible models to explain our results, with an emphasis on the localized acoustic oscillator that, we think, encompasses all the observations made so far. We conclude with a short outlook.

2. Experimental

Anthracene (Aldrich, scintillation grade, 99.0% purity) was further purified in a home-built zone-refiner for about 4000 passes. 7.8,15.16-dibenzoterrylene (DBT) was purchased from Dr W Schmidt (Laboratory for PAH Research, Greifenberg, Germany). Samples were single crystals of anthracene as the host, doped with DBT as the guest. Flat crystals (flakes) were grown by cosublimation in a home-built device under a 150 mbar nitrogen atmosphere. This cosublimator consisted of a large tube (30 mm diameter) containing a load of anthracene powder and heated by resistant wires. Crystals grew on a collector plate at a slightly lower temperature than the load. Within the sublimator, a small crucible containing the guest, DBT, was heated with resistant wires wrapped around it, up to an adjustable temperature. We could thus control the concentration of probe molecules in the matrix. The sublimation flakes developed along the (a, b) plane and reached diameters of a few millimeters and thicknesses of a few micrometers.

The substrates of the structures consisted of either glass plates for control experiments, or, for the majority of measurements, Si wafers highly p-doped with boron (with a resistivity of 0.001–0.01 Ω cm). The wafers were coated with a thermally grown, 400 ± 20 nm thick layer of SiO_2, on top of which interdigitated gold electrodes with spaces of 5, 10 or 20 μm were deposited by e-beam lithography (substrates made by the Fraunhofer-Institut für Mikroelektrische Systeme und Schaltungen, Munich, Germany). For the early experiments, the electrodes were often treated with a 10 mM solution of nitrobenzenethiol in acetonitrile before mounting the crystal. This treatment significantly reduces the contact resistance, which helps charge injection and improves electrical conduction at low temperature [16]. We later omitted this treatment, because strong charge injection can suppress the resonances described hereafter or make them unobservable. The anthracene crystals were then optically contacted to the gold electrodes on the structures, and cooled down in a pumped helium bath cryostat. The lowest temperature we could achieve was 1.4 K. A schematic drawing of our anthracene FET structure is presented in figure 1(a). For some experiments, we applied a weak mechanical bending stress to the substrate by means of a piezoelectric bimorph actuator (not shown).

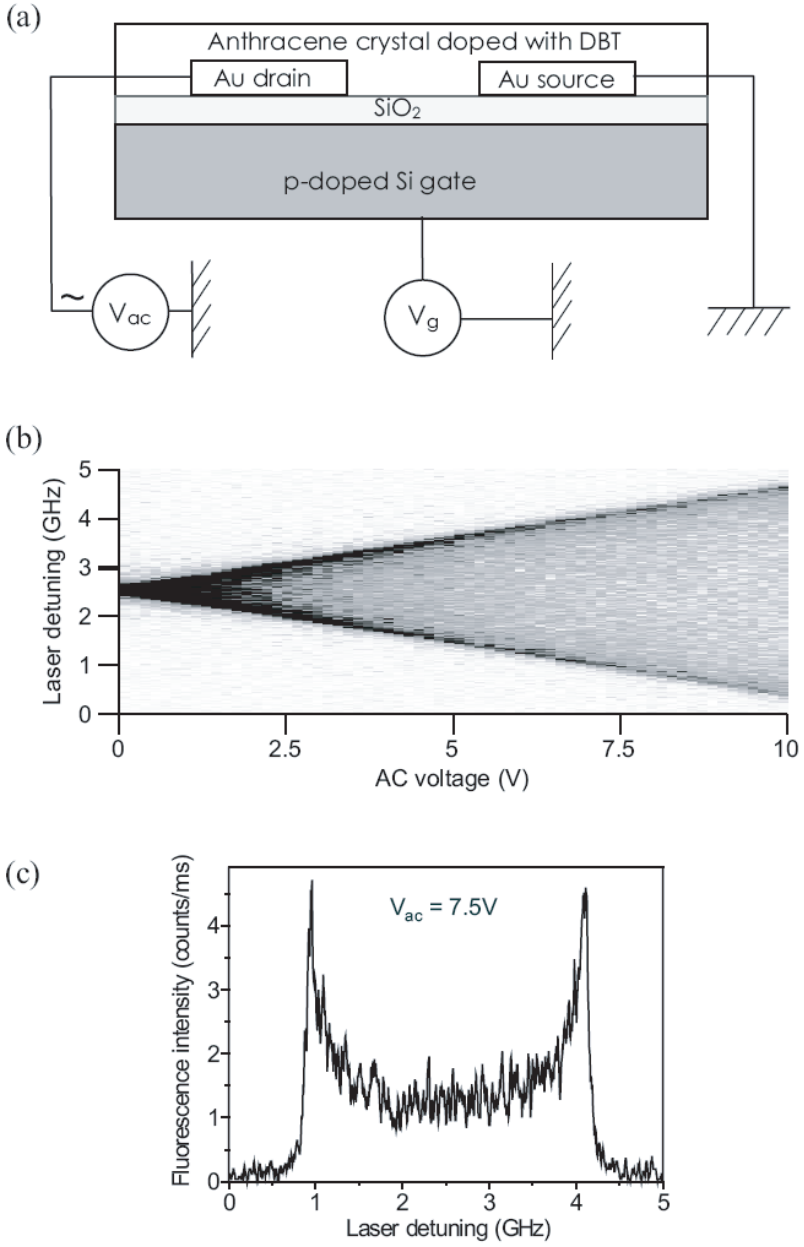

Figure 1. (a) Electrical scheme of the FET samples used for the experiments. An anthracene single crystal is contacted to (interdigitated) gold electrodes deposited on 400 nm of silica grown on a heavily p-doped silicon substrate used as the gate electrode. Ac voltages (from 1 mV to at most 100 V) are applied to the drain contact. (b) An example of the linear Stark effect on the optical line of a single DBT guest molecule. The optical excitation spectrum is scanned vertically, whereas the amplitude of the applied ac voltage is scanned, here between 0 and 10 V, at a constant frequency of 10 kHz. The fluorescence intensity is coded as a level of gray. (c) Cross-section spectrum of (b) at a voltage amplitude of 7.5 V, displaying the characteristic 'cat's ears' profile of the SM line, with enhanced intensity at the voltage turning points.

The SM measurements were performed with a home-built confocal microscope [3, 4]. Briefly, the samples were illuminated with a single-frequency Ti-sapphire laser (Coherent 899–21) pumped by an argon ion laser (Coherent Innova 200). The tightly focused laser beam (diameter: about 1 μm) was brought onto the surface of the single crystal, with the beam axis perpendicular to the (a, b) plane, by means of a microscope objective (60×, NA = 0.85, Edmund Optics). The whole objective and the sample holder were immersed in superfluid helium. A fast steering mirror (Newport FSM-300-01) outside the cryostat allowed us to move the focused beam in the plane of the sample over an area of about $200 \times 150\,\mu\text{m}^2$. Fluorescence was detected after suitable long-pass filters (810 nm, Chroma), which blocked the residual laser light and transmitted much of the fluorescence. Fluorescence excitation spectra were obtained by scanning the laser frequency over the molecular resonance lines of DBT and recording the fluorescence signal from a digital avalanche photodiode (SPCM-AQR-15, PerkinElmer).

The temperature-dependent measurements on the system were performed in the range 1.4–2.1 K by monitoring the temperature with a calibrated resistor (Cernox Resistor CX-1050-AA-1.4L, LakeShore, Westerville, OH). Our bath cryostat did not allow us to independently vary the temperature and pressure.

Time-resolved fluorescence signals for discrete 'sparse' Fourier transform (SFT; see below) analysis were obtained with a special data acquisition card (TimeHarp 200) with a maximum time resolution of 300 ns.

3. Results

We investigated the fluorescence excitation spectra of different individual DBT molecules in anthracene FET structures under an applied ac voltage. Because of the relatively large capacity of the transistor chip, we could not apply frequencies larger than 10 MHz. Using FETs as substrates instead of simple electrodes on glass slips (without a gate electrode) allowed us to achieve higher electric fields in the organic crystal. In a glass slip, the electric field is distributed between the electrodes (separated by 5–20 μm), whereas in the FET structure, a much stronger electric field is concentrated between the source/drain electrodes and the gate, separated by a very thin oxide layer (0.4 μm). Another advantage of the FET structure is the possibility of varying the concentration of charge carriers in the anthracene crystal and to study the role of these charges in the observed phenomena. Some of the experiments were repeated on glass slips without a gate electrode and gave similar results (taking into account lower values of the electric field and smaller concentrations of charges in the latter case). Unless stated otherwise, all experiments reported in this paper were done with a fixed gate voltage of −40 V.

When a weak ac voltage $V_0 \cos \Omega t$ is applied at a low frequency to the electrodes, the lines of SMs located between the electrodes shift periodically at the applied frequency due to the Stark effect [6]. If the static dipole moments in the ground and excited states are different, the Stark effect will be linear and the optical transition frequency will oscillate sinusoidally at the frequency Ω (see figure 1(b)). When both the molecule and its insertion site in the matrix are centrosymmetric, both static dipole moments are zero, and the Stark effect, which then arises from the difference in polarizability between the ground and excited states, is much weaker and purely quadratic. The optical line shifts sinusoidally at frequency 2Ω asymmetrically to one side of the unperturbed transition. In both cases, however, the steady-state spectrum results from a time average of the shifting line, and shows two intense structures corresponding to the turning points of the voltage, at $-V_0$ and V_0 (or at 0, $\pm V_0$ for a purely quadratic Stark shift), and a

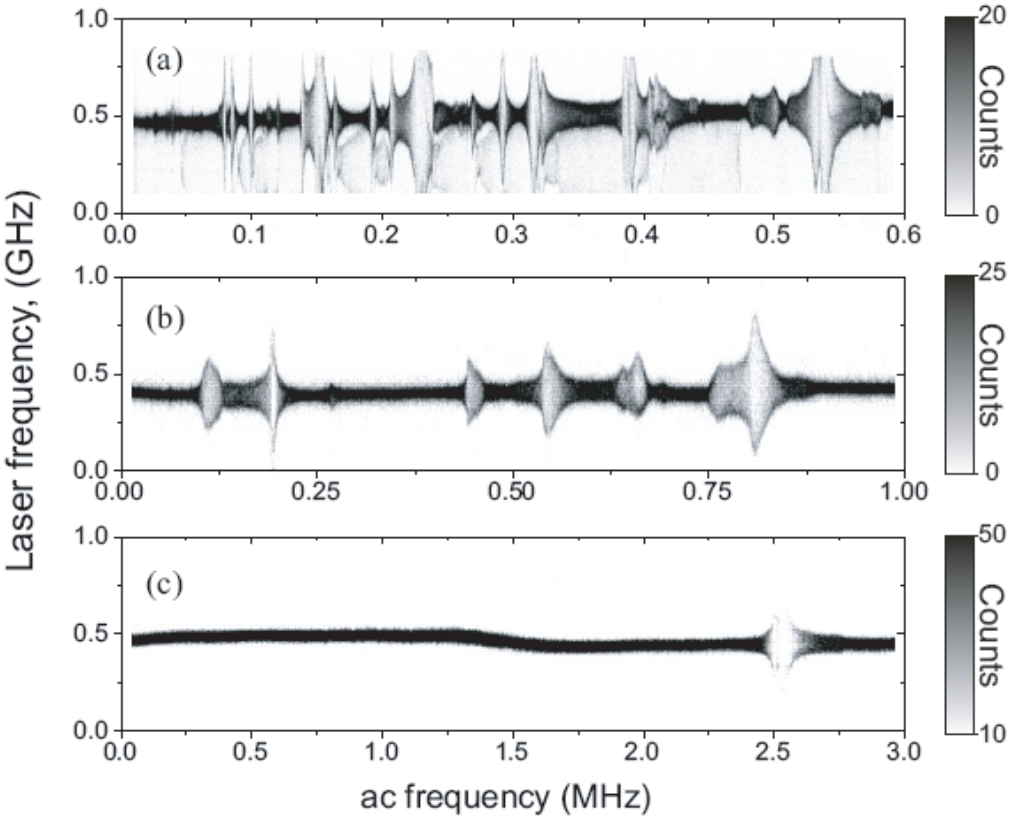

Figure 2. Examples of resonance spectra obtained for three different molecules in different samples. The spectra vary from simple (c) to very complex (a). Resonances are distributed between some tens of kHz and a few MHz (the upper frequency attainable was limited by the capacitance of our FET structures). Note the wide distribution of shapes and widths, and the general correlation of frequency and width (low-frequency resonances are narrower). The gray scales on the right indicate the number of fluorescence counts per pixel.

minimum between those 'cat's ears' [14, 15]. An example of such a spectrum is presented in figure 1(c). More complex profiles arise when both linear and quadratic components of the shift are present at the same time.

Molecules situated far from the electrodes are not directly exposed to the field. Therefore, we expected their spectral lines to be almost purely Lorentzian, even at high applied voltages. However, the lines of these molecules showed surprisingly large resonant splittings for certain ac frequencies in a range between several kHz and several MHz. These resonances were observed over a rather large area, 70 μm or more away from electrodes, in places where the applied electric field was practically negligible. Figure 2 shows typical response curves of different SMs. The number of resonant frequencies in the range 0–10 MHz found in an SM trace may vary from zero or one to several tens. The lowest resonances are found between 10 kHz and 10 MHz, depending on the specific crystal, its mounting and its thermal history. For example, molecule (a) in figure 2 has several tens of resonances with frequencies less than 600 kHz, whereas molecule (c) has only two close resonances (at 2.65 and 2.7 MHz) in a much wider

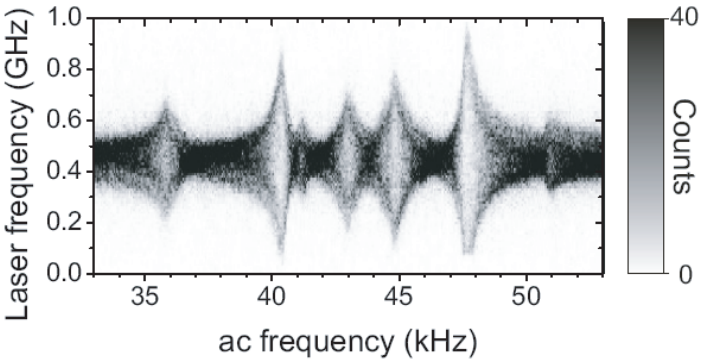

Figure 3. Example of the 'multicomponent' structure of a resonance in the range from 33 to 53 kHz. For a high applied voltage, these resonances appear to merge into a single broad peak. At weak enough voltage, we observe discrete resonances with frequencies 35.8, 40.3, 41.2, 43, 44.8, 47.5 and 50.8 kHz and respective quality factors 44, 89, 205, 85, 99, 79 and 112. The number of counts per pixel is indicated in the gray scale on the right.

range (up to 3 MHz). Moreover, in addition to several main frequencies Ω_i, we often observed sub-harmonic and harmonic resonances at about $\Omega_i/2$ and $2\Omega_i$ and, at large enough ac voltages, still higher harmonics (see below) and combinations of them. The resulting pattern can be extremely complex.

In high-quality sublimation-grown crystals, a similar pattern of resonances is observed for all the SMs within a rather large area (see below). The same resonant modes were observed for many days consecutively in the same sample, with occasional shifts of the resonance frequencies to slightly different values (often higher ones) when the temperature was raised above $\sim$100 K during the night. Usually, the resonant frequencies of different DBT molecules at the same spot in the sample were identical in the two spectroscopic sites (main site and red site [5]). Less often, we found slight but clear differences between resonances in these two sites. The observed resonance frequencies are affected neither by the intensity nor by the polarization of the exciting laser.

Some of the resonances appear rather broad at a large applied voltage, but resolve into several components when the voltage amplitude is reduced. An example of a 'multi-component' structure in a resonance is shown in figure 3. This 'multi-component' appearance is rather different from the fine structure of electronic states in atoms or molecules. As is obvious from the plot, the components at the different frequencies appear to belong to different oscillators. They could be assigned neither to an inhomogeneous mixture of systems with different oscillation frequencies (only one molecule is observed!) nor to jumps of an oscillator between different conformational states with different frequencies (no such jumps could ever be detected, even in multiple recordings of the same trace).

Figure 4(a) shows a $150 \times 150\ \mu m^2$ confocal microscope image of an anthracene crystal placed on a substrate with two 10 μm-spaced gold electrodes, recorded at 1.4 K. One can easily see cracks in the anthracene crystal. These cracks relax the stress accumulated in the structure upon cooling because of the shrinkage of anthracene, which is larger than that of silicon. For all the molecules located in the same microcrystal, within the boundaries defined by the cracks, we found common resonance frequencies in their responses to the ac voltage, usually with

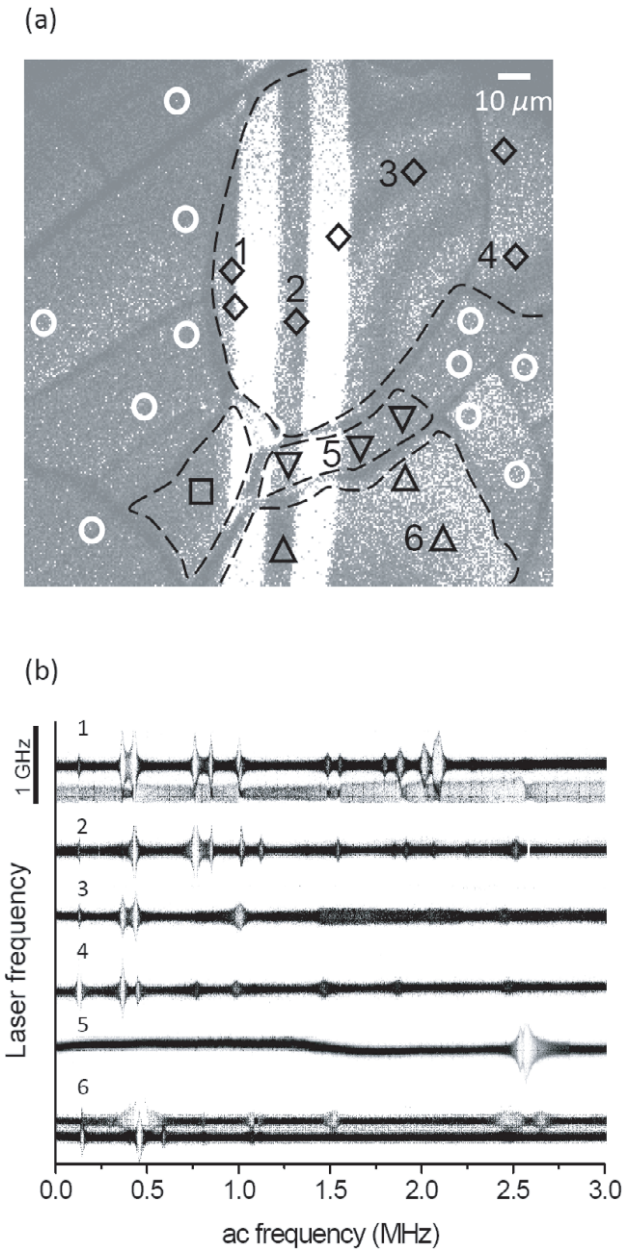

Figure 4. Spatial correlation of the resonance spectra measured on different molecules. The same resonances are usually found for all the molecules within a microcrystal. Often, the resonance amplitude remains large, even several tens of microns away from the exciting electrodes (see trace number 4), where the applied electric field is negligible. This observation shows that the direct Stark effect is not the main mechanism responsible for the resonance, but agrees well with interaction of the molecule with a delocalized acoustic deformation field. The correlation of resonance spectra over large distances in anthracene single crystals is in marked contrast with the short correlation lengths observed in polycrystalline Shpol'skii matrices [14, 15], and points to the influence of crystal defects and crystal quality on the resonance phenomenon.

different intensities from molecule to molecule. In figure 4(a), the white circles indicate the SMs that show no resonant response under a variable ac frequency. The black symbols of a given type indicate the SMs that presented resonances at common frequencies, with possibly different intensities. As can be seen, every microcrystal presents its own characteristic spectrum of resonances, provided it has some part exposed to the field in between the electrodes. Note that the resonances are equally pronounced for molecules far from the space between electrodes. Usually, cracks appear to isolate crystal parts with different resonance spectra, but the same resonant pattern can occasionally be observed on both sides of a crack (compare molecule 4 with molecules 1–3). Smaller microcrystals generally present resonances at higher ac frequencies (see molecule 5). We performed similar measurements using a spin-coated polycrystal of anthracene [17] instead of a high-quality sublimation flake. In this polycrystal, each microcrystal (several microns in size) situated between electrodes presented a different pattern, and all SMs within the microcrystal showed the same pattern. The lowest frequencies in these microcrystals were usually higher than 2 MHz.

We found a very strong dependence of the amplitude and width of the resonances on temperature. Figure 5(a) shows typical traces of one and the same molecule, measured at 1.4, 1.7 and 2.1 K. One sees that even a modest increase of temperature, from 1.4 to 2.1 K, increases the broadening of the resonance by a factor of 5–10 and decreases its amplitude by a factor of more than 10. Figure 5(b) shows temperature dependences of widths and amplitudes for some of the most intense resonances. We fitted power laws T^{α} to these dependencies, with an exponent between -5 and -10 for the amplitude of the resonance, and an exponent between 4 and 7 for its width. We have to keep in mind, however, that the range of temperatures explored is extremely narrow and that Arrhenius or other dependences might fit the data as well. We also found a slight decrease of the resonance frequency with increasing the temperature (1–10% frequency reduction for different modes from 1.4 to 2.1 K). Another remarkable observation is that, at a given temperature, the width of each resonance appears to correlate with the frequency of resonance. At $T = 1.4$ K we observed a roughly linear correlation between the width of a resonance and its frequency (see figure 6). The frequency/width ratio (or quality factor) was about 100. Note that the width of resonances increased markedly with the amplitude of the applied voltage. Although most of the above widths were measured at voltages as low as possible (empty circles in figure 6), some points measured at high voltages (full triangles) may lie significantly above the correlation line.

In addition to the main modes (frequencies Ω_i), we often observed sub-harmonic ($\Omega_i/2$) and harmonic ($2\Omega_i$) resonances. Figure 7 (top) shows an intense resonance at $\Omega = 415$ kHz, which is isolated at low voltage and can be attributed to the fundamental frequency of a given oscillator. At higher voltages, we find a resonance at 207 kHz (equal to $\Omega/2$) and another one at 813 kHz, close to $2\Omega = 830$ kHz. Two additional resonances appeared at 755 and 909 kHz and they cannot be easily related to Ω, and probably belong to other modes. The trace of the same molecule measured at a still higher ac voltage (figure 7, bottom) reveals other structures, which appear in the vicinity of frequencies $\Omega/4$, $3\Omega/4$ and $5\Omega/4$. Such a behavior suggests a strong anharmonicity of the oscillating system. The classical theory of nonlinear mechanical oscillators predicts resonances at a frequency $\Omega_{res} = p/q\,\Omega_0$, where p and q are integers (see, for example, [18]); however, the intensity of the resonance phenomena quickly decreases with p and q.

Another indication of the nonlinear nature of these resonances is the typical variation of the resonance's lineshape with increasing amplitude of the driving force (see figure 8). For small

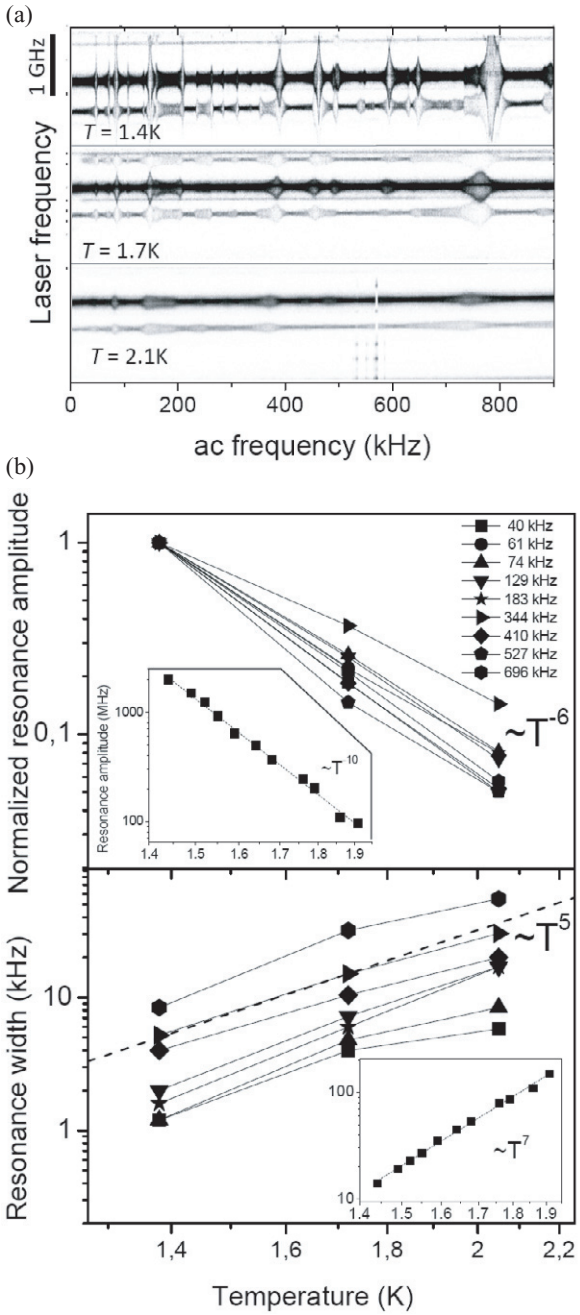

Figure 5. Temperature dependence of the resonances. (a) At the lowest measurement temperature, 1.4 K, the resonances are very sharp (quality factor: about 100). An increase in temperature leads to a very fast broadening of the resonances and to a dramatic reduction of their amplitude for a given voltage. (b) Examples of the temperature dependence of the amplitude (top) and the width (bottom) of the resonances, for a group of resonances taken in the same spectrum. The insets show more temperature points measured on one particular molecule/resonance. The data in the insets have been fitted by power laws of temperature.

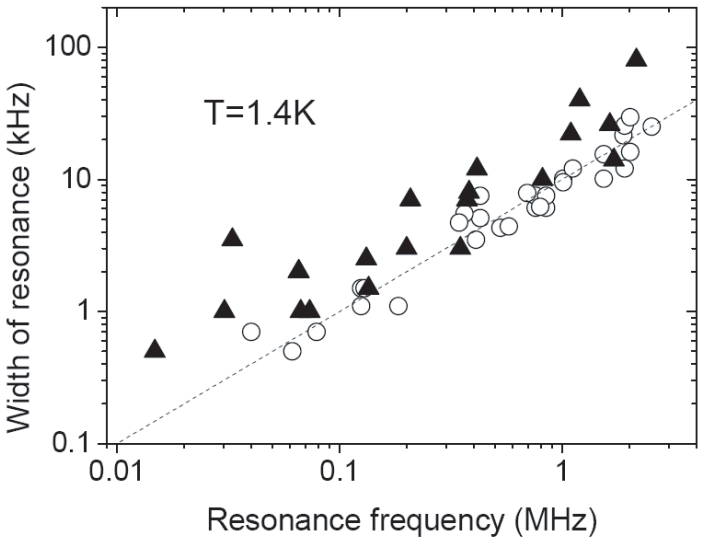

Figure 6. Correlation between width and frequency of several resonances, measured on various molecules and samples at 1.4 K. The empty circles correspond to resonances measured at very small voltages. The full triangles have been measured irrespective of the applied voltage, and some of them may be broadened by voltage saturation. Note that all points are around or above the dotted line, corresponding to a quality factor of about 100.

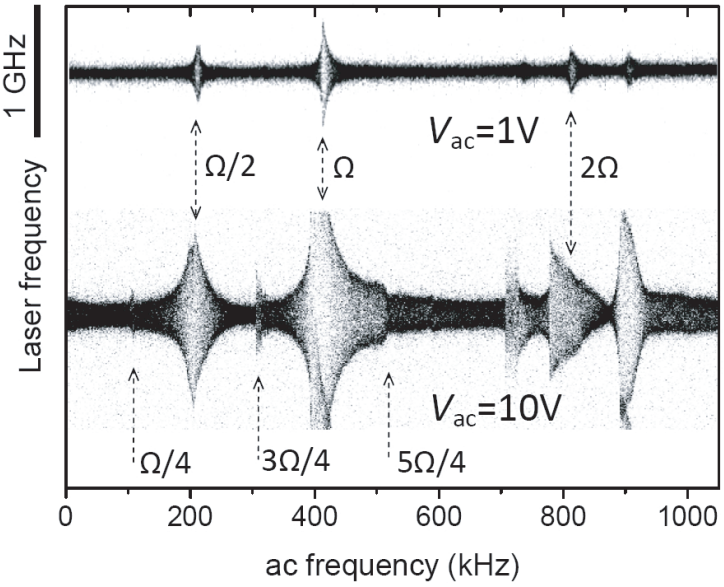

Figure 7. Appearance of multiples and fractions of a main frequency as the amplitude of the driving voltage increases, from 1 V (top) to 10 V (bottom). This points to strong nonlinear, anharmonic effects.

enough V_{ac} the resonant curve presents almost symmetrical low- and high-frequency wings. However, increasing the amplitude V_{ac} leads to a shift of the resonance frequency and to a substantial deformation of the shape of the resonance. For a decrease of the resonance frequency with the amplitude (negative anharmonic coefficient), the resonance shape would show a smooth increase of the amplitude on approaching the resonance from above, with a discontinuous jump to a smaller amplitude in the vicinity of the low-amplitude resonance. If the frequency is now scanned upwards and the resonance is approached from below, the amplitude of the oscillation jumps suddenly to a larger value at a frequency higher than that of the previous jump. Such a hysteretic behavior is characteristic of anharmonic oscillators [18], and can be clearly seen in the experimental traces of figure 8, scanned with increasing (top) or decreasing (bottom) the ac frequency.

In order to check the anharmonic nature of the observed oscillations and to test the linearity of the response, we studied the dependence of the oscillation amplitude at the main frequency Ω, at $\Omega/2$ and at 2Ω. As it was important to avoid any saturation and anharmonic frequency shifts, we had to use the smallest driving ac voltage possible, still giving a measurable effect on the optical SM line. To do so, we propose the following original method, inspired by the working of a lock-in amplifier. We tune the frequency of the exciting laser to one of the wings (roughly at half-maximum) of the fluorescence excitation spectrum of a molecule and apply a small ac voltage to the electrodes at the desired frequency (e.g. that of the resonance or its (sub)harmonic). We then record a real-time fluorescence time trace with high temporal resolution ($\sim$300 ns) with the Time-Harp data acquisition card. The resulting time trace contains oscillating components at the frequency of interest, or at its (sub)harmonics. We then perform a discrete Fourier transform analysis of the obtained time trace, which, for low enough frequency, reveals the periodicities in input data as well as the relative strengths of any periodic components (figure 9(a)). As the data set required for a Fourier transform is too 'sparse' for high frequencies, we call this analysis SFT. With this procedure, it proves possible to detect line shifts much smaller than the optical linewidth of DBT (about 40 MHz), corresponding to applied voltages of a few millivolts, and to fields of a few hundreds of $V\,m^{-1}$ only.

Figure 9(b) shows the dependence of the oscillation amplitude on the applied voltage, determined by using the SFT. The amplitude of the main mode Ω (=48.1 kHz) excited at resonance depends linearly on V_{ac} (except for a slight saturation for large voltages) in full agreement with that of a linearly excited oscillator at resonance. We also observed such a linear dependence by directly measuring the line splitting at resonance as a function of voltage, at much higher ac voltages, up to 10–15 V. For still higher voltages $V_{ac} < 50$ V, the excited amplitude showed a sublinear dependence, indicating the onset of a saturation mechanism. For the ac frequency 23.9 kHz ($\approx\Omega/2$), the SM line shift has two oscillating components, one with the driving frequency $\Omega/2$ (with an amplitude proportional to V_{ac}, as expected from linear response theory), and one at the resonant frequency Ω. The amplitude of this latter oscillation is proportional to V_{ac}^2, as expected for a second-order excitation of the main resonance. This process is comparable with second-harmonic generation in nonlinear optics. The resonant part of the shift around $\Omega/2$ arises from this latter effect only, and therefore appears for high enough V_{ac} only. Finally, we also probed the oscillation amplitude at 98.3 kHz ($\approx 2\Omega$) by the SFT and a direct measurement of the spectrum, and found a linear dependence on V_{ac}. This indicates that the oscillation at 2Ω is another resonant mode and does not correspond to the excitation of the oscillation at Ω by a nonlinear parametric coupling [18].

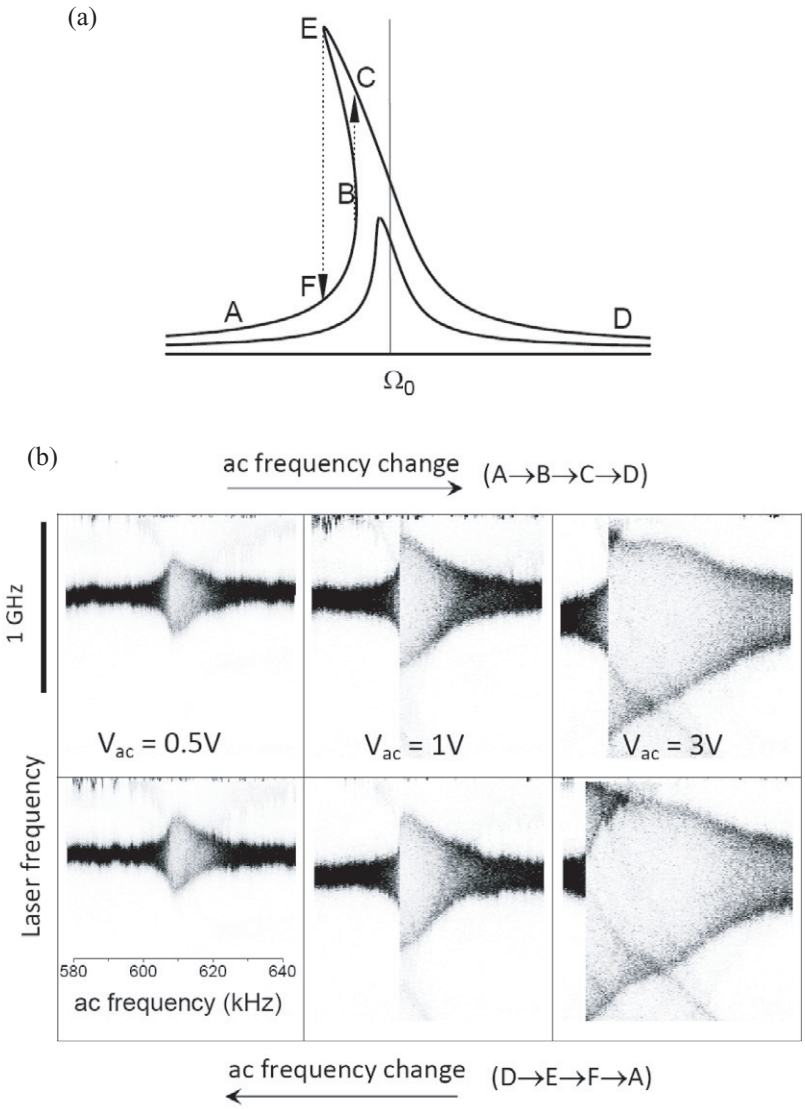

Figure 8. Anharmonic hysteresis behavior. (a) Due to anharmonicity, the resonance frequency decreases when the amplitude of the oscillation increases. Because of this frequency shift, the resonance signal is bi-stable in a narrow region below the resonance [18]. This behavior is indeed observed on the resonances when the voltage frequency is scanned upward (trace A → B → C → D and top part of panel (b)) or downward (trace D → E → F → A and bottom part of panel (b)). The hysteresis appears for about 0.7 V and its amplitude increases when the applied voltage increases to 3 V.

Finally, we tested the effect of a mechanical deformation of the substrate and of the attached crystal by applying a voltage to a piezoelectric bimorph actuator. The stresses applied were comparatively low (about 1 atm, as deduced from the optical shift of SM lines), but led to clear shifts of the resonance frequencies by about 1% in relative value.

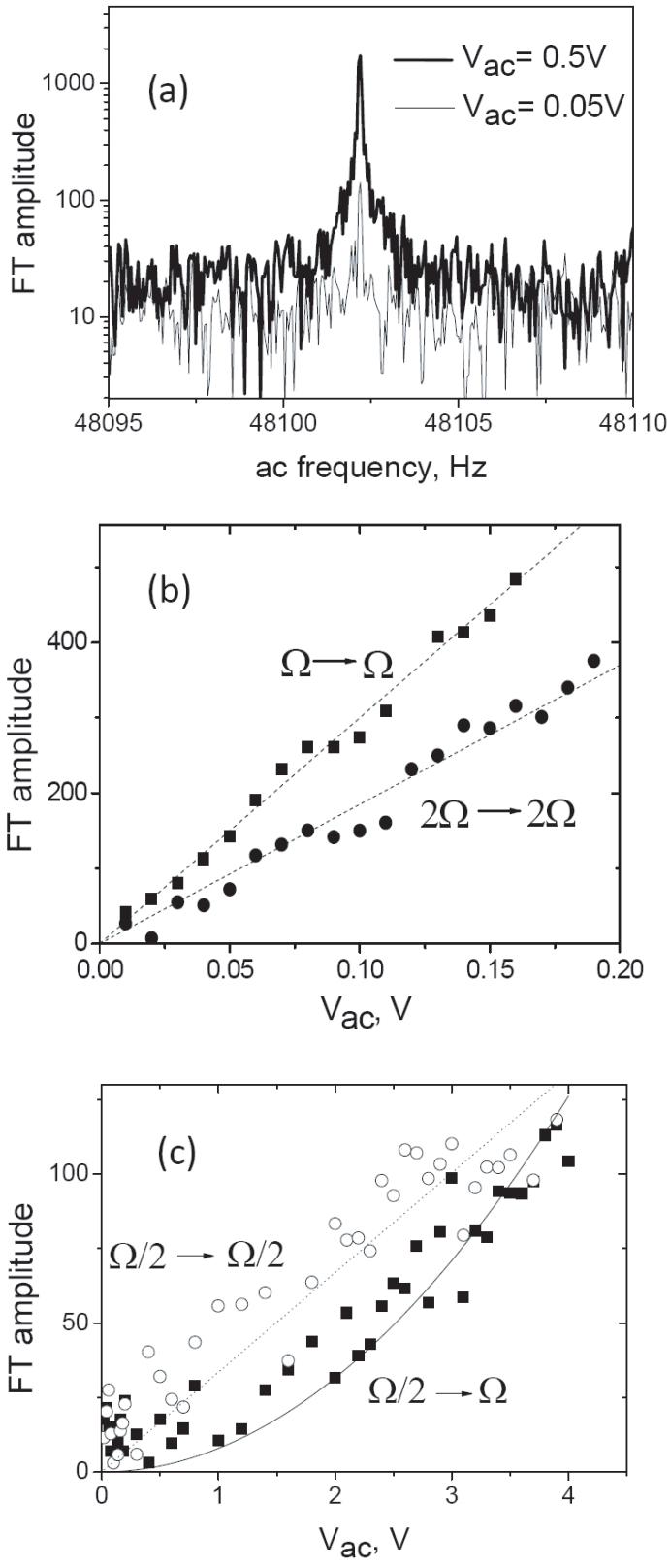

Figure 9. Caption on next page.

Figure 9. Fine analysis of the dependence of the resonance amplitude on the voltage applied, with a sparse Fourier transform scheme (see text for explanations). The top panel shows the noise spectrum in the optical intensity signal upon application of weak voltages. The central peak arises from the intensity modulation by the frequency modulation of the optical SM line. The modulation is still clear for applied voltages as low as 50 mV. The middle panel (b) shows that the modulation is linear in applied voltage for the main resonance Ω (noted $\Omega \rightarrow \Omega$, squares), as well as for the resonance at about the double frequency (resonance slightly shifted from 2Ω, denoted by $2\Omega \rightarrow 2\Omega$, circles). This excludes a parametric excitation mechanism for the latter mode. For excitation at half the frequency of the main resonance, $\Omega/2$ (panel (c)), the oscillation amplitude at the main resonance frequency Ω is quadratic in applied voltage (denoted by $\Omega/2 \rightarrow \Omega$, squares), whereas the oscillation at the excitation frequency $\Omega/2$ is obviously linear (denoted by $\Omega/2 \rightarrow \Omega/2$, empty circles).

4. Discussion

In a perfect dielectric insulator, the probe molecules are only affected by the local electrostatic field from polarization charges, as there are no free charge carriers to move around. The standard coupling mechanism between a molecule and an applied electric field in such a material is the linear and quadratic Stark shift [6]. Because the local field at a low temperature is expected to arise mainly from electronic polarization, it should respond extremely rapidly to changes in applied voltage. Both the linear and quadratic Stark effects have been observed for single dye molecules in solid matrices, and indeed have been found to respond quasi-instantaneously at frequencies of several hundreds of MHz [6]. The regular Stark effect therefore cannot explain our observations.

More complex optical shift mechanisms can take place in conducting materials, where charges can be transported and accumulated with a profound influence on local electric fields. In these systems a rich variety of interaction mechanisms was observed [10, 11, 14]. Electric forces acting on moving or trapped charges can further lead to new coupling mechanisms involving perturbations of the SM's environment by changes in temperature, pressure or strain, etc. In the following, we examine some possible mechanisms by which the observed ultra-low-frequency resonances might arise.

4.1. Helium bubble vibrations

High electric fields can inject charges into liquid helium, creating charged He bubbles where Coulomb repulsion is balanced by the liquid's surface tension [19]–[22]. As such bubbles carry a charge, they are susceptible to ac fields that can excite resonant shape oscillations. The strong temperature dependence of our resonances at first sight seems to suggest that the superfluid helium bath might be involved in the phenomenon. However, several observations rule out this interpretation. The most natural place to form He bubbles would be at the anthracene–helium interface of each microcrystal. We therefore covered our sample with a thick polymer (PMMA) layer (several tens of microns) to prevent contact with the liquid helium bath. We observed the same qualitative behavior as in the uncovered sample, which rules out a direct involvement of He bubbles. Moreover, the temperature dependence of the resonances does not agree with any

of the simple properties of liquid helium in this range of temperature. From these arguments, we conclude that helium bubbles are not involved in the resonances.

4.2. Electrical oscillations of a system of charges or currents

Similar resonances of the ac Stark shift have already been reported for very different host–guest systems, terrylene and tetra-tert-butyl-terrylene (TBT) guests in a polycrystalline n-hexadecane host, itself deposited on a highly conducting indium–tin–germanium oxide (ITGO) film [14, 15]. In this work, a droplet of a solution of terrylene or TBT molecules in toluene was spread on the semiconductor ITGO film. After the toluene had evaporated, a small quantity of n-hexadecane was spread on the surface, allowed to evaporate for several minutes to reduce its thickness, and then quickly cooled in the cryostat. A large fraction of the impurity molecules were thought to remain stuck to the semiconductor surface or located at a very short distance from it. Under an applied ac voltage, strong resonances of the optical line splitting of single TBT molecules were also found, with frequencies ranging from a few kHz to below 1 MHz. The main difference from our observations was that the ac resonance spectrum (including frequency, width and intensity) depended on the particular molecule under study, even within the same laser spot (about 1 μm in diameter). Therefore, the correlation length of the oscillators was considerably shorter than in the present work, probably well below 100 nm, as no two molecules presented the same resonance spectrum. Caruge and Orrit [14, 15] have proposed two possible explanations for the resonances, which both involve the motion of charges in the semiconductor. A first line of thought is the resonating phenomena observed at low frequencies over large areas (a few millimeters) in doped semiconductors at low temperatures. These phenomena are thought to arise from spatial and temporal instabilities in current filaments [23]. A second model would involve localized recharging waves in compensated semiconductors [24, 25]. Recharging waves arise from exchanges of charge carriers between the free carrier gas and traps in the semiconductor lattice. Because the trapping rates can be low (times longer than milliseconds), these waves can propagate at very low velocities, and could lead to localized resonances with extremely low frequencies.

These two models are based on purely electrical dynamics of charge carriers in a highly conducting material. It is difficult to generalize them to the (relatively) poorly conducting anthracene crystal. Moreover, as the conduction properties of the crystal are strongly modulated by the gate voltage, we expect that changes in gate voltage would have a dramatic influence on the dynamics of the charge carriers. Because we never observed any significant influence of the gate voltage on the frequency of the oscillators (although the oscillation amplitude usually increased significantly for large positive or large negative bias), we rule out oscillator models based on charge dynamics only. Our observations therefore suggest that none of the explanations of Caruge and Orrit [14, 15] are correct.

4.3. Mechanical or localized acoustic oscillations

Excluding models based on pure charge carrier dynamics, however, does not mean that charges have no part in the observed phenomena. The possibility of injection and motion of charge carriers at the interface between the conductor and insulator appears to be an important requisite in the phenomenon. Indeed, in highly insulating matrices, such as n-dodecane, we failed to observe any resonance of the Stark effect of single DBT molecules, even for high applied

fields. In [14, 15], the resonances were observed for dye molecules dissolved in an insulating hexadecane matrix, but a large fraction of the dye molecules was thought to lie close to or at the semiconductor surface. Therefore, in this configuration too, injection and trapping of charges in an insulator (hexadecane) from a conductor (ITGO) may have occurred on a short range.

We have seen that the resonance has a large amplitude, even far away from the electrodes, in areas where the applied electric field is negligible (compare the oscillation amplitude for molecules 1 and 2, situated close to the electrodes and, for molecule 4, very far away from the electrodes in figure 4). This again confirms that the oscillation does not arise from a simple Stark effect. The large coherence length of the oscillation (several tens of microns) rather suggests a delocalized, mechanical or acoustical vibration of the whole lattice of the microcrystal. Note that a localized standing acoustic wave in the microcrystals under study can in no way match the observed frequency. With a sound velocity of about $3000\,\mathrm{m\,s^{-1}}$, a typical crystal size of $10\,\mu\mathrm{m}$ would lead to a very high resonance frequency of about 300 MHz.

Optical zero-phonon lines are very sensitive to the pressure or strain field of an acoustic wave [26]. We can easily imagine mechanisms by which such acoustic oscillations would be excited. Injected charges and charge distributions in the crystal lattice and at various interfaces, defects or cracks can respond to electric forces from the applied voltage. Because these charges are trapped or confined by impurities, interfaces or defects in the crystal, they can transmit mechanical action to the lattice. One can envision them as the anchorage points that allow us to apply electrical external forces locally to the lattice. If the applied ac frequency is close to the frequency of a standing wave mode in the crystal or of some other localized acoustic mode, resonant oscillations will be excited. The ensuing delocalized strain field leads to a periodic shift of SM optical lines, which act as sensitive microphones. Such an electric–vibrational coupling may be considered as an inverse piezoelectric effect, where mechanical stress–strain can be produced by an applied electric field. Although the guest, the crystal and the insertion site are all centrosymmetric [4, 5], the symmetry breaking required for a piezoelectric effect can be induced by defects. Because the damping of oscillations by the acoustic phonon bath becomes very inefficient at low temperatures, these driven oscillations can reach amplitudes large enough, not only to be observed, but even for anharmonicity and other nonlinear effects to become important.

Our working hypothesis in the rest of this discussion is the latter model of a mechanical vibration of the whole microcrystal, extending over zones as large as some tens of micrometers in single-crystalline sublimation flakes. Localized acoustic modes in homogeneous anthracene microcrystals (longitudinal and transverse sound velocities: 3 and $2\,\mathrm{km\,s^{-1}}$) with sizes of $\sim 30\,\mu\mathrm{m}$ should have frequencies of ~ 100 MHz, considerably higher than the resonances we observed. However, much lower frequencies can be obtained if stress is concentrated in small regions or around weak contacts between crystal parts. The fundamental oscillation of a tuning fork is a good example of such a low-frequency localized mode. In a tuning fork, the large mass of the arms is moved by the weak spring of the U- or hinge region, leading to a frequency much lower than the ratio of the sound velocity to the dimension of the fork. In other words, stress is mostly concentrated in the hinge region of a tuning fork, whereas displacement is more distributed. From this argument, we expect that smaller microcrystals will tend to lead to higher frequencies.

Another general trend is that thin crystals tend to present lower-frequency resonances than thick ones, with higher frequencies in spin-coated anthracene than in sublimation flakes. One could imagine low-frequency vibrations as bending modes of a thin crystal partially stuck to the substrate (some images indeed suggest partial contact between the crystal and substrate,

see the area around molecule 3 in figure 4(a)). This hypothesis, however, cannot be absolutely general. In the experiments of [14, 15] showing very low resonance frequencies, the thin layer of hexadecane matrix was applied to the semiconductor surface as a thin wetting liquid film. Modes with frequencies as low as some hundreds of Hz should rather be explained by defects and weak contacts between microcrystal grains. Hereafter, we briefly speculate on the possible relation of our low-frequency vibration modes to other known low-frequency modes.

Amorphous materials (glasses, polymers and polycrystals) are known to present excess degrees of freedom at low temperatures with respect to single crystals. Beyond saturable two-level systems [27], quasi-local vibration modes (QLMs) occur normally in disordered solids [28, 29]. Even a small concentration of defects in a crystal can introduce additional normal modes and modify the pattern of the atomic displacements. These additional localized or quasi-localized modes give rise to an excess density of states of phonons at low frequencies, appearing in Raman scattering spectra at frequencies lower than $10\,\mathrm{cm}^{-1}$ (GHz–THz range). This vibrational anomaly of glasses and other disordered systems is known as the boson peak [29]–[31]. For each particular sample, the individual low-frequency resonances we detect can be interpreted as localized modes in the extreme low-frequency tail of the boson peak. Maksimov and Kaznov [32] have proposed that microcracks or other defects in a crystal can give rise to localized vibrational modes. Simple pictures of such a mode could be a surface Rayleigh wave localized in a ruptured area, or a whispering gallery acoustic mode around the boundaries of a microcrystal. Intrinsically localized modes (ILMs) can arise from a lattice distortion combined with anharmonicity, as proposed by Sievers and Takeno [33, 34]. These modes can, in principle, occur anywhere in the lattice, and could be thermally induced, but they could also be pinned to structural defects and persist down to low temperatures.

Hereafter, we discuss how the model of a localized acoustical lattice vibration fits our observations in section 3. In this model, SM lines shift mainly because of the oscillating strain field in the lattice. We thus expect a general linear dependence on the oscillation coordinate instead of the more complex dependence of the Stark effect (linear and quadratic components), depending on the particular molecule. Of course, in between the electrodes both effects contribute, leading to more complex patterns, as observed.

The requirement of localized charges to apply forces to the lattice agrees well with our observation that the amplitude of the vibration usually increases with the gate voltage in the FETs. This requirement also explains why we observe no resonance in insulating materials upon application of electric fields. Electrostrictive effects are weak and piezo-electric coefficients are nil in centrosymmetric crystals. Charge injection could have occurred in the hexadecane/ITGO experiments [14] close to semiconductor grains, and definitely takes place in our anthracene FET. Anthracene is a conducting crystal, into which positive charges are injected from gold electrodes, and which can store or conduct charges to trapping regions.

As mentioned previously, the observed resonance frequencies are not compatible with standing acoustic waves, but could arise from soft or deformed regions of the crystal. The delocalization of the acoustic stress field to a whole anthracene microcrystal is not surprising for a low-frequency mode, as the image of the tuning fork suggests. The correlation lengths were much shorter in the case of polycrystalline hexadecane on ITGO, although the frequencies were as low as in anthracene, which suggests that the soft points could be the grain boundaries between microcrystals. Crystallinity thus seems to correlate well with the spatial extent of the modes, but not necessarily with their frequencies.

The splitting of a mode into several lines at high resolution ('multi-component' structure) is difficult to understand as coupling of an oscillator to a multistate system, because we never observed jumps of the oscillation frequency between different values. A possible interpretation of this splitting could be the anharmonic modulation of one oscillator by even slower ones (see figure 3), creating side bands split by the slow modulation frequencies.

At the fixed temperature of 1.4 K, we observe a strong linear correlation between the frequency of a mode and its width (the quality factor is constant). Similar dependences of the width on frequency were observed for the quartz oscillators used as reference clocks. The damping of these oscillators has been fitted with a sum of linear and quadratic dependences on frequency in the GHz range [35] with high-quality factors. In the MHz range, the linear term largely dominates, leading also to a constant quality factor when the frequency is varied. Similar results were obtained in $LiNbO_3$ resonators, with quality factors as small as 200 at 847 MHz [36]. When the temperature is raised, the amplitude of the resonance decreases and its width increases dramatically. This indicates a very efficient damping of the vibrations by thermal phonons, reminiscent of the damping of low-frequency acoustic waves in insulating crystals. The mechanism of this process was suggested by Akhiezer [37], who modeled the absorption of sound waves in crystals with heat flow and viscous damping. A sound wave passing through a crystal causes a disturbance of the thermal Planck phonon population. The ensuing relaxation produces entropy and removes energy from the sound wave, thus damping it. This mechanism leads to a fourth-power temperature dependence (T^4) of the damping rate, and to a square dependence of this rate on the frequency for vibrational modes at low temperatures [36, 38, 39]. Akhiezer's damping agrees well with the temperature dependences we observe for the width and amplitude of the oscillations. However, the linear correlation of the width with frequency is more difficult to explain.

Finally, the resonant oscillations we found present clear signatures of anharmonicity and of nonlinearity. We observed the resonance frequency to decrease at large applied voltages when the vibration amplitude increases, a common occurrence in molecular oscillators. The quadratic excitation of a mode at half its resonance frequency is a clear manifestation of nonlinearity also attributable to anharmonicity of the oscillation potential. Further work is needed to understand the behavior at very large amplitudes, where more and more harmonics and subharmonics appear. Another clear signature of anharmonicity is the hysteretic jumping observed as the driving frequency is tuned continuously through the resonance. The hysteresis follows from the anharmonic variation of the resonance frequency with the amplitude of lattice oscillations. We can relate the anharmonicity parameter to the vibration amplitude if we remark that the optical shift of the SM line in response to a hydrostatic stress is about 1 GHz atm^{-1}. The relative frequency shift of 1% that we measured (about 6 kHz out of 600 kHz, see figure 8(b)) corresponds to the measured optical shift of 1 GHz and therefore to a stress of about 10^5 Pa. We could achieve comparable shifts of the optical and vibrational frequencies by deforming the piezoelectric actuator attached to the substrate. It therefore appears that the anharmonicity found in our resonances is significantly larger than that of a purely acoustic oscillation. For an acoustic phonon, the applied stress should be compared with the compression and shear moduli of the crystal, about several GPa. For a modest stress of 1 atm, one would thus expect a relative frequency shift smaller than 10^{-4}, two orders of magnitude smaller than the shift we measure. In other words, a local deformation in the low-frequency resonant mode appears to concentrate the stress on a very small crystal volume (in the tuning fork picture, this volume would correspond to the hinge region).

5. Conclusion

In this paper, we have reported ultra-low-frequency resonances when an ac voltage with a variable frequency is applied at liquid-helium temperatures to a molecular single crystal contacted to a silicon substrate. Those resonances were detected by the shift of the optical transitions of single guest molecules, which act as local nanoprobes. The various experiments reported here consistently point to a mechanical or acoustical origin for these resonances, which the molecules pick up as nanomicrophones (or 'nanophones'). The oscillations appear to be excited by the applied electric field through electric forces on charges injected in the material, and trapped at defects, cracks and interfaces. The electric conduction properties of the crystal are therefore crucial to obtain and understand the excitation of those resonances. These localized low-frequency modes appear to be closely related to the resonances previously observed with SMs in an organic–semiconductor composite system [14, 15]. Therefore, the tentative attribution of these older observations to a purely electrical effect was probably incorrect.

All of our observations can be understood and rationalized within the hypothesis of electrically excited mechanical oscillations, in particular the low frequency of the vibrations, their anharmonicity, the sign (alternating between positive and negative) and the linear nature of the optical shift, the persistence of this shift for molecules far away from the regions with high electric field, and the steep temperature dependence, indicating a strong coupling to thermal phonons.

To the best of our knowledge, such localized low-frequency modes have not been detected earlier in bulk measurements. There may be several explanations for this. The large distribution of frequencies in polycrystalline samples makes it impossible to isolate a single mode in a bulk experiment. Moreover, it is difficult to inject charges in a uniform way in a massive sample. Because SMs probe local areas, where only a few modes can be active, they can pick up single local oscillators, much as they pick up tunneling motions of single two-level systems in glasses [30, 40, 41] or higher frequency quasi-local modes [29, 42].

The observation of these low-frequency resonances leaves many questions open. The exact nature of the vibrating coordinate is unknown. Acoustic oscillations with frequencies in the kHz–MHz range have wavelengths ranging from 3 m to 3 mm. By which mechanism are such low-frequency modes concentrated in the few tens of microns found here, or even in a few tens of nanometers, as found at the ITGO surface [15]? In order to study them in more detail, one would have to create and isolate these oscillators in a more controlled way. A possible route would be the creation of reproducible defects in a crystal, by a controlled mechanical deformation. The amplitude of the vibration could then be mapped out as a function of position by monitoring the lines of a number of SMs distributed across the sample.

Finally, beyond their scientific interest as models for nanomechanical devices, one can ask whether these low-frequency modes could be useful. They could be examples of localized vibrations in solids, which are difficult to access with bulk techniques. Another intriguing question is their quality factor, which appears to increase very steeply at low temperatures. In the absence of any other damping mechanism, the quality factor could become as high as 1 million at 50 mK. Such fine resonances could be used for many experiments in much the same way as quartz tuning forks are used for scanning probe microscopy.

Acknowledgments

This work was part of the European research project CHIC (contract no. IST-2001-33578) and of a research program of a Stichting voor Fundamenteel Onderzoek der Materie, which is part of the NWO. MK acknowledges support from the Russian Foundation for Basic Research (07-02-00547).

References

[1] Moerner W E and Orrit M 1999 *Science* **283** 1670
[2] Plakhotnik T, Donley E A and Wild U P 1997 *Annu. Rev. Phys. Chem.* **48** 181
[3] Hofmann C, Nicolet A, Kol'chenko M A and Orrit M 2005 *Chem. Phys.* **318** 1
[4] Nicolet A A L, Hofmann C, Kol'chenko M A, Kozankiewicz B and Orrit M 2007 *ChemPhysChem* **8** 1215
[5] Nicolet A A L, Bordat P, Hofmann C, Kol'chenko M A, Kozankiewicz B, Brown R and Orrit M 2007 *ChemPhysChem* **8** 1929
[6] Brunel C, Tamarat P, Lounis B, Woehl J C and Orrit M 1999 *J. Phys. Chem.* A **103** 2429
[7] Moerner W E and Kador L 1989 *Phys. Rev. Lett.* **62** 2535
[8] Kador L, Latychevskaia T, Renn A and Wild U P 2000 *J. Lumin.* **86** 189
[9] Kador L, Latychevskaia T, Renn A and Wild U P 1999 *J. Chem. Phys.* **111** 8755
[10] Bauer M and Kador L 2002 *J. Lumin.* **98** 75
[11] Bauer M and Kador L 2003 *J. Chem. Phys.* **118** 9069
[12] Nicolet A A L, Hofmann C, Kol'chenko M A and Orrit M 2008 *Mol. Cryst. Liq. Cryst.* **497** 218–27
[13] Nicolet A A L 2007 Single-molecule probes in organic field-effect transistors *PhD Thesis* Leiden
[14] Caruge J M and Orrit M 2001 *Phys. Rev.* B **64** 205202
[15] Caruge J M and Orrit M 2002 *J. Lumin.* **98** 1
[16] Gundlach D J, Jia L L and Jackson T N 2001 *IEEE Electron Device Lett.* **22** 571
[17] Pfab R J, Zimmermann J, Hettich C, Gerhardt I, Renn A and Sandoghdar V 2004 *Chem. Phys. Lett.* **387** 490
[18] Landau L D and Lifshitz E M 1976 *Course of Theoretical Physics* vol 1 *Mechanics* (London: Pergamon)
[19] Volodin A P, Khaikin M S and Edel'man V S 1977 *JETP Lett.* **26** 543
[20] Albrecht U and Leiderer P 1987 *Europhys. Lett.* **3** 705
[21] Tempere J, Gladilin V N, Silvera I F and Devreese J T 2007 *J. Low Temp. Phys.* **148** 181
[22] Tempere J, Silvera I F and Devreese J T 2007 *Surf. Sci. Rep.* **62** 159–217
[23] Brandl A and Prettl W 1991 *Phys. Rev. Lett.* **66** 3044
[24] Kazarino R F, Suris R A and Fuks B I 1972 *Sov. Phys. Semicond.* **6** 500
[25] Kazarino R F, Suris R A and Fuks B I 1973 *Sov. Phys. Semicond.* **7** 102
[26] Ambrose W P and Moerner W E 1991 *Phys. Rev.* B **43** 1743
[27] Phillips W A 1972 *J. Low Temp. Phys.* **7** 351
[28] Maradudin A A, Montroll E W and Weiss G H 1963 *Theory of Lattice Dynamics in the Harmonic Approximation* (*Solid State Physics* suppl. vol 3) ed F Seitz and D Turnbull (New York: Academic)
[29] Vainer Y G, Naumov A V and Kador L 2008 *Phys. Rev.* B **77** 224202
[30] Phillips W A (ed) 1981 *Amorphous Solids: Low Temperature Properties* (Berlin: Springer)
[31] Esquinazi P (ed) 1998 *Tunneling Systems in Amorphous and Crystalline Solids* (New York: Springer)
[32] Maksimov I L and Kaznov D P 2002 *Solid State Commun.* **121** 305
[33] Sievers A J and Takeno S 1988 *Phys. Rev. Lett.* **61** 970
[34] Takeno S and Sievers A J 1988 *Solid State Commun.* **67** 1023
[35] Campbell C 1989 *Surface Acoustic Wave Devices and Their Signal Processing Applications* (New York: Academic) p 124

[36] Habti A El, Bastien F, Bigler E and Thorvaldsson T J 1996 *J. Acoust. Soc. Am.* **100** 272
[37] Akhiezer A 1939 *J. Phys.* (*USSR*) **1** 277
[38] Woodruff T O and Ehrenreich H 1961 *Phys. Rev.* **123** 1553
[39] Bömmel H E and Dransfeld K 1960 *Phys. Rev.* **117** 1245
[40] Boiron A M, Tamarat Ph, Lounis B, Brown R and Orrit M 1999 *Chem. Phys.* **247** 119
[41] Naumov A V, Vainer Y G and Kador L 2007 *Phys. Rev. Lett.* **98** 145501
[42] Vainer Y G, Naumov A V, Bauer M and Kador L 2006 *Phys. Rev. Lett.* **97** 185501